

Local environment of Nitrogen in $\text{GaN}_y\text{As}_{1-y}$ epilayers on GaAs (001) studied using X-ray absorption near edge spectroscopy

J. A. Gupta^[*],¹ M. W. C. Dharma-wardana,¹ A. Jürgensen,² E.D. Crozier,³ J.J. Rehr,⁴ and M.Prange⁴

¹ *Institute for Microstructural Sciences, National Research Council of Canada, Ottawa, Canada K1A 0R6*

² *Canadian Synchrotron Radiation Facility, Madison WI, 53589-3097 USA*

³ *Dept of Physics, Simon Fraser University, Burnaby, Canada V5A 1S6*

⁴ *Dept of Physics, University of Washington, Seattle, WA 98195-1560 USA*

(Dated: September 21, 2018)

X-ray absorption near-edge spectroscopy (XANES) is used to study the N environment in bulk GaN and in $\text{GaN}_y\text{As}_{1-y}$ epilayers on GaAs (001), for $y \sim 5\%$. Density-functional optimized structures were used to predict XANES via multiple-scattering theory. We obtain striking agreement for pure GaN. An alloy model with *nitrogen pairs* on Ga accurately predicts the threshold energy, the width of the XANES “white line”, and features above threshold, for the given X-ray polarization. The presence of N-pairs may point to a role for molecular N_2 in epitaxial growth kinetics.

PACS numbers: 61.10.Ht, 81.15.Hi, 71.15.Mb

Nitrogen-alloyed GaAs, i.e., $\text{GaN}_y\text{As}_{1-y}$, is intensely studied owing to its technological importance. Even very small amounts of N lead to a dramatic y -dependent decrease in the bandgap[1]. In the ultradilute regime ($y < 0.01\%$), localized, single-impurity levels produce sharp resonances above the GaAs conduction band minimum. With increasing y , small nitrogen aggregates (pairs and higher clusters) give rise to localized states in the band gap, producing sharp photoluminescence (PL) lines [2, 3]. At higher concentrations ($y > 0.1 - 0.25\%$), the sharp PL lines merge to a broader line. Anomalous bandgap bowing and other effects are observed [2, 4] in this regime. At these concentrations, a phenomenological band anti-crossing model works well [5, 6], since here the details of N-incorporation seem to be unimportant. Kent and Zunger[4] presented a theoretical study using pseudopotentials and large supercells containing various N-atom configurations. In reality, a plethora of different local atomic environments is possible, since Ga can have 0 to 4 first neighbour N atoms; N pairs can have different orientations or separations; and triplets or higher order clusters are possible [4, 7]. The change in PL on annealing has even been attributed to the removal of N interstitials or defect complexes, such as N-As split interstitials [8, 9].

Several groups have used XANES to study local atomic structures in GaNAs epilayers. Lordi *et al.*[10] modeled their N XANES data using local densities of states (LDOS) obtained from the Vienna *Ab Initio* Simulation Package(VASP) [11]. For GaNAs the partial LDOS did not reproduce the experimental “white line” and predicted several unobserved oscillatory features above the absorption edge. Simpler tight-binding (TB) methods have also been examined by other authors [13]. In general TB is unreliable except for band-structure type calculations[14] to which the TB parameters have been fitted.

In this Letter we present a study of N incorporation

in $\text{GaN}_y\text{As}_{1-y}$ epilayers. Our objectives are: (i) to compare the local nitrogen environments in the dilute nitride and in bulk GaN; (ii) to predict the XANES spectra for several local atomic arrangements of N in $\text{GaN}_y\text{As}_{1-y}$ and compare them with experiment. These calculations used the *ab-initio* code FEFF8 [15] which combines simultaneous real-space full multiple scattering (FMS) calculations of near-edge X-ray absorption spectra within a self-consistent field (SCF) treatment of the electronic structure. The microscopic structure of the alloy epilayers for N or (N,N) pair-configurations were separately determined via density-functional theory (DFT) using the VASP code[11] within an ultrasoft pseudopotential scheme, and the generalized gradient approximation for the exchange-correlation potential. The DFT optimized structure was used as the input to the XANES calculations. The predicted XANES spectra are in very close agreement with the experimental results, and support the presence of (N,N) pair clusters in this alloy regime ($y \sim 3 - 6\%$).

The single, uncapped $\text{GaN}_y\text{As}_{1-y}$ epilayer used here was grown by solid-source MBE as described elsewhere[16]. The actual composition, $y = 0.0496$, and thickness, 333 Å, of the sample were obtained from high-resolution X-ray diffraction data via dynamical diffraction analysis. A thick, metalorganic vapor phase epitaxy-grown GaN layer on sapphire (0001) was used as a reference. Experimental XANES measurements were performed at the Canadian Spherical Grating Monochromator beamline of the Synchrotron Radiation Center at the University of Wisconsin, Madison. The storage ring energy was 1 GeV, and a 600 lines/mm grating was used. The measurements on GaN and GaNAs epilayers used entrance-slit widths of 100 μm and 250 μm , providing energy resolution of ~ 0.24 eV and 0.54 eV, respectively. Measurements at the nitrogen K-edge were performed using both total electron yield (TEY) and total fluorescence yield (TFY) modes of detection. TEY provides

more surface-sensitive information. For GaN, the TEY and TFY data were nearly identical, but the TEY data exhibited a more intense main peak. For GaNAs, only the TFY data are presented here. The samples were out-gassed by *in-situ* heating to 280 °C for ~ 4 hours in the ultra-high vacuum analysis chamber. The effectiveness of this surface preparation was evident from the elimination of the Oxygen K-edge peak in the absorption spectra.

Five $\text{GaN}_y\text{As}_{1-y}$ models were considered in this study. For each structure, state-of-the-art DFT calculations within the generalized gradient approximation (GGA) were carried out with a 64 atom $2 \times 2 \times 2$ supercell of zincblende unit cells, with periodic boundary conditions. Tetragonal distortions were included by holding the in-plane epilayer lattice constant at the GaAs(substrate) value. The lattice constant along the growth direction and atomic positions were relaxed until the Hellman-Feynman forces became negligible, resulting in the lattice constant along the growth direction being smaller than the in-plane value. Each FEFF model was formed by “stacking” 27 relaxed DFT supercells to form a 1792-atom, cubic supercell with the absorbing-N atom at the center. Spherical clusters using only the 295 central atoms were used for the FEFF calculations. A single N atom in the DFT cell yields the alloy concentration $y = 1/32$. The artificial periodicity of the DFT supercell resulted in second N atoms at ~ 11.2 Å from the central, “quasi-isolated” N absorber. All our models contain this artificial periodicity. Using the notation of Ref. 4, we also considered (N,N) pairs in m th nearest neighbour positions with $m=1, 2$ and 6, corresponding to FCC lattice positions $(1/2 \ 0 \ 1/2)$, $(1 \ 0 \ 0)$ and $(\bar{1} \ 1 \ \bar{1})$. For the $m=2$ case, we studied (N,N) pairs parallel ($m=2a$) or perpendicular ($m=2b$, $(0 \ 0 \ \bar{1})$) to the substrate, with the X-ray absorbing atom at $(0 \ 0 \ 0)$. Thus, we have one “single N” model, and four (N,N) pair models labeled as NN*m*, i.e.,

Single N, NN1, NN2a, NN2b and NN6 (1)

For nitrogen K-edge XANES, large FEFF clusters are needed to capture multiple scattering resulting from the high density and the long mean free path resulting from the very long core-hole lifetime (inverse lifetime = 0.116 eV). In this work, 27 and 295-atom SCF and FMS clusters were used and parallel-processed on 32 nodes.

Fig. 1 shows the experimental data for the thick GaN reference epilayer obtained at incidence angles of 0° and 45°, relative to the surface normal. The data show a rich fine structure consistent with previous reports [17, 18]. These two data sets illustrate the importance of polarization effects, (cf. Ref. 17). Most notably, the peaks near 402.5 eV and 406.8 eV are significantly enhanced at 45° compared to normal incidence. The former is close to the “magic” angle, 54.7° (the Lambert angle), where the polarization effects would be completely suppressed [18].

The figure also shows the FEFF8 results for the GaN N K-edge XANES based on the hexagonal Wurtzite

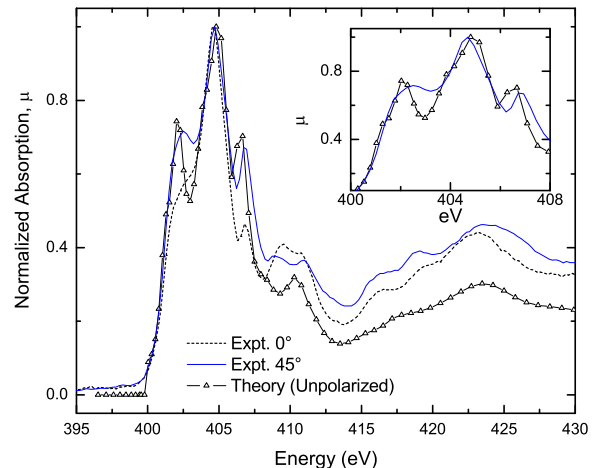


FIG. 1: Nitrogen K-edge XANES for wurtzite GaN compared with theory (unpolarized calculation). Incidence angles of 0° and 45° were used in single scans at a rate of 10 sec/point, and step size of 0.25 eV. The inset shows the excellent agreement for incidence at 45°, close to the Lambert angle.

structure with the unit cell parameters $a = 3.186$ Å, $c = 5.178$ Å. Clearly, the theory is very successful in predicting the main XANES features, especially at 45°. In particular, the edge energy is accurately predicted without any “fitting” to experiment. The experimental absorption edge energy, $E_0 = 401.1 \pm 0.1$ eV was determined from the zero of the second derivative of the absorption, while the value $E_0 = 400.93$ eV was predicted by FEFF. The experimental uncertainty is about half the energy step (0.25 eV). On normalizing to match the height of the main peak, ~ 405 eV, the theory accurately predicts the magnitudes and positions of the peaks near 402.5, 406.8 and 411 eV, as well as the local minimum near 414 eV, the local maximum near 423 eV, and the general decay of the absorption with increasing photon energy. A determination of the experimental polarization was difficult given the irregular shape of the sample after cleaving the sapphire substrate. Hence the appropriate comparison is between our unpolarized model and the experimental data at 45°. Unlike the theoretical results of Ref. 17, our results show no overestimate of the peak positions at higher energies. This suggests that the multiple-scattering methods of FEFF8 can be used for $\text{GaN}_y\text{As}_{1-y}$ with confidence, if a realistic alloy structure is available.

Fig. 2 shows the experimental XANES for the $\text{GaN}_y\text{As}_{1-y}$ epilayer. The local environment of the Nitrogen in the alloy is clearly different from the pure GaN. The absorption threshold in this case has a single, narrow “white line”, as opposed to the multiple peaks in GaN. A smaller, distinct peak is observed at 402.3 eV, coincident with the lowest energy peak in pure GaN. The top panel shows that the NN1 model accurately predicts

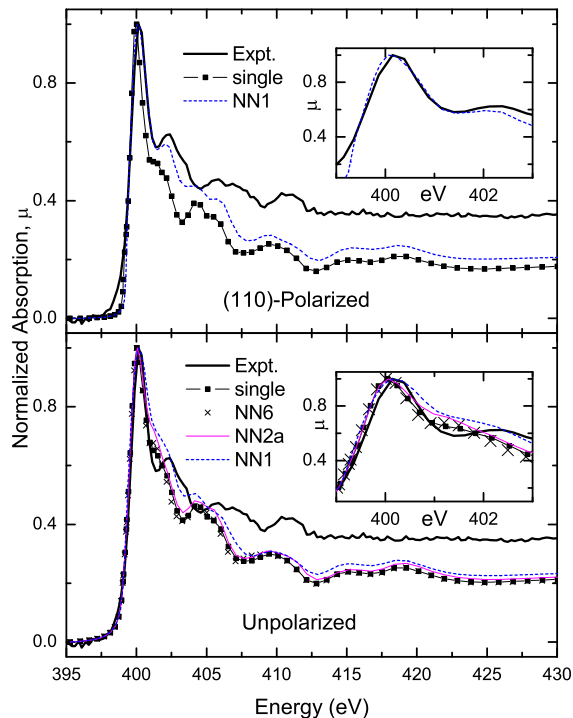


FIG. 2: Nitrogen K-edge XANES for a coherently-strained GaNAs epilayer (thick line) compared with theoretical models listed in Eq. 1. The data are single scans, with 135 sec/point, and a step size of 0.25 eV. Top: for photons polarized along (110). Bottom: unpolarized photons. The XANES for NN2b is very similar to NN2a, and is omitted. The theoretical absorption asymptote for higher eV is lower than in experiment as self-absorption effects are not included in the theory.

the first and second peaks when the photon polarization is included in the theory. The lower panel shows that the unpolarized calculation may have some relevance to the threshold edge, and for energies above ~ 405 eV. The threshold energy was found to be $E_0 = 399.6 \pm 0.1$ eV. Our experimental data are consistent with those in Refs. 10 and 13. The data of Ref. 12 are similar, although their second peak intensity is almost at the “white line”.

Several properties determined from the DFT calculations are summarized in Table I. The DFT predicted tetragonal distortions are in agreement with Vegard’s law, confirming its applicability in this alloy regime.

For the single-N atom model, the Ga-N bond lengths are nearly identical, $R = 2.0567$ Å, while the NN1 model predicts a distribution of bond lengths, $R = 2.072 \pm 0.042$ Å. This is an indication of lattice distortions produced by this configuration, and we find that this (N,N) pair configuration is not as energy optimal [4] as some other models. However, Molecular Beam Epitaxy is a non-equilibrium technique hence the MBE-grown epilayer need not have the most energy-optimal N-cluster. The objective of the XANES is in fact to find the most

TABLE I: Growth direction (001) lattice constants a_{\perp} , and average Ga-N bond lengths b with standard deviation σ_b , and nearest nitrogen distance R obtained by total energy minimization for the alloy models (see Eq. 1 in the text) studied here. N.B., the Ga-N and Ga-As bond lengths in cubic GaN and GaAs are 1.9500 and 2.4480 Å, respectively. The in-plane lattice constant is constrained to the GaAs value, 5.6534 Å.

| Model | a_{\perp} (Å) | b (Å) | σ_b (Å) | R (Å) |
|----------|-----------------|---------|----------------|---------|
| Single N | 5.5865 | 2.0567 | 0.0002 | 11.1730 |
| NN1 | 5.5131 | 2.0722 | 0.0416 | 3.6908 |
| NN2a | 5.5108 | 2.0504 | 0.0010 | 5.6530 |
| NN2b | 5.5195 | 2.0510 | 0.0007 | 5.5191 |
| NN6 | 5.5087 | 2.0468 | 0.0010 | 9.7066 |

prevalent N cluster in the alloy sample prepared via MBE.

Fig. 2, bottom panel illustrates the spectral changes due to the local N environment in the singlet and pair models, not including polarization effects. In this figure the FEFF8 spectra were shifted (by an amount smaller than the experimental stepsize 0.25 eV) to match the experimental edge energy. The threshold energy E_{th} is almost identical for the different models, and hence independent of the local bonding configurations and the number of N atoms in these models. The shift in the E_{th} between GaN and $\text{GaN}_y\text{As}_{1-y}$ (-1.45 eV) is thus a general feature of N alloying in GaAs, and is related to long-range effects and the larger lattice constant of the $\text{GaN}_y\text{As}_{1-y}$ epilayer compared with GaN. This is consistent with the concept of nitrogen impurities forming “perturbed host states” in GaAs [4].

The apparent discrepancy between the calculated intensities at higher energies compared with the experimental results is due to a reduced white line intensity in our fluorescence data due to self-absorption effects; our normalization using this lower peak intensity causes the apparent increase in the absorption at higher energies. Otherwise, the “white line” is reproduced extremely well by FEFF, and is not affected by the local nitrogen environment. The XANES white line is often understood as arising from a high density of final states or exciton effects due to the Coulomb interaction between the photoelectron and the core hole [19]. Nodwell *et al.* suggested that the white line is due to a N-related resonance in the conduction band and not to an excitonic bound state [13]. However, core hole effects were included in our FEFF calculations and provide an excellent description of the data.

The NN6 model and the single-N atom model have very similar spectra (Fig. 2, bottom panel), indicating that the phase interference between the two atoms with the large NN6 separation is sufficiently small as to have no effect on the XANES, in agreement with the negligible

interaction energy for $m = 6$ pairs (see also Ref. 4). In the models where the second N atom is moved closer to the N absorber, the interaction as well as interference of scattered amplitudes becomes more significant. For the NN2 models interactions produce a slight increase in the intensity of the high-energy shoulder near the white line, but the rest of the NN2a and NN2b spectra are similar to the single and NN6 models. A more dramatic effect is observed for the NN1 model. The intensity of the shoulder is increased and the shoulder is shifted closer to the small peak at 402.3 eV of the experimental data. All models predict a minimum near 413 eV, well-aligned with the falling edge of the final experimental peak. The predicted features between 413 eV and about 419 eV are common for all models and similar to those in GaN in this energy range. These spectral features are due mostly to Ga-N bonds, traditionally studied by EXAFS.

We return to the polarized photon calculation of Fig. 2. The absorption cross-section depends on the components of atomic bonds along the direction of the electric field polarization. For the NN1 pair model, the NN1 neighbour is located at (2.6438Å, 0.000Å, 2.5753Å), so the (110) and ($\bar{1}$ 10) components are approximately equal. The agreement between theory and experiment is strong evidence that NN1 pairs are responsible for the peak at 402.3 eV in the experimental data. We also note that the 402.3 eV peak is not shown by the other models and is not well-resolved in several triplet models (see Ref. 4) that we examined, but have not reported in detail in this paper. If the tetragonal distortion (coherent epilayers) arising from fixing the in-plane lattice constant to the substrate is relaxed, the resulting “annealed” NN1 model loses the 401.4 eV minimum (fig.2 top panel shows only the coherent epilayer results) and the 402.3 eV peak moves to lower energies and becomes a shoulder. This type of peak narrowing is expected since the annealing reduces the bond-length distribution. In fact, the width of the 402.3 eV peak in the experimental data (fig.2, top) as compared to the theory suggests that the samples have more disorder than in the optimal tetragonal NN1 model used in the theory.

Nodwell *et al.* noted that their XANES data were the same for samples with different N compositions [13]. This seems reasonable since the observed fine structure contains major contributions from microscopic N aggregates, such as nitrogen first-neighbour FCC pairs, and these structures are formed even at very low N content. Ref. 4 considered several triplet structures, including the Cs symmetry triplet proposed by Gil and Mariette [20], which was found to be consistent with GaNP data. The cluster formation does not result solely from the natural, statistical distribution of N atoms. The low miscibility of N in GaAs has been suggested as a cause of locally ordered structures [21, 22]. An interesting possibility for the origin of close N,N pairs is that they are favoured by the kinetics of the epitaxial growth process. In fact, it

has recently been proposed that molecular nitrogen in an excited state is a dominant agent in GaN MBE.[23]

In conclusion, high-resolution XANES of a coherently-strained $\text{GaN}_y\text{As}_{1-y}$ epilayer on GaAs(001) and a bulk GaN film were presented. For pure GaN, our theoretical spectrum agrees extremely well with the measured spectrum and demonstrates the effectiveness of the full multiple scattering approach within the self-consistent field calculations of the Fermi energy, and the importance of the synchrotron polarization. For the strained $\text{GaN}_y\text{As}_{1-y}$ epilayer on GaAs(001), the calculated spectra exhibited a strong sensitivity to the local N environment and we show that nitrogen FCC *pairs* attached to Ga captures the observed XANES.

Acknowledgements- We thank Z.R. Wasilewski for useful comments, D. Ritchie for computer-system help, M. Tomlinson and S. Moisa for technical support, and H. Tang for the GaN reference sample. CSRF is funded by the National Research Council of Canada and an MFA grant from the Natural Sciences and Engineering Research Council of Canada (NSERC). SRC is funded by the U.S. National Science Foundation under grant No. DMR-0084402. One of us (EDC) acknowledges funding from an NSERC Discovery Grant.

-
- [1] S.H. Wei and A. Zunger, Phys. Rev. Lett. **76**, 664 (1996).
 - [2] S. Francoeur et al., Appl. Phys. Lett **75**, 1538 (1999).
 - [3] X. Liu, M.-E. Pistol and L. Samuelson, Phys. Rev. B **42**, 7504 (1990).
 - [4] P.R.C. Kent and A. Zunger, Phys. Rev. B **64**, 115208 (2001).
 - [5] W. Shan et al., Phys. Rev. Lett. **82**, 1221 (1999).
 - [6] E.P. O'Reilly and A. Lindsay, Phys. Stat. Sol. B **215**, 131 (1999).
 - [7] P.R.C. Kent et al., Appl. Phys. Lett. **79**, 2339 (2001).
 - [8] P. Krispin et al., Appl. Phys. Lett, **80**, 2120 (2002).
 - [9] S.B. Zhang and S.-H. Wei, Phys. Rev. Lett. **86**, 1789 (2001).
 - [10] V. Lordi et al., Phys. Rev. Lett. **90**, 145505 (2003).
 - [11] G. Kress, J. Furthmuller and J. Hafner, see <http://cms.mpi.univie.ac.at/vasp/>
 - [12] V.N. Strocov et al., Phys. Stat. Sol. (b) **233**, R1 (2002).
 - [13] E. Nodwell et al., Phys. Rev. B **69**, 155210 (2004).
 - [14] N. Tit and M. W. C. Dharma-wardana, App. Phys. Lett. **76**, 3576 (2000)
 - [15] A.L. Ankudinov, B. Ravel, J.J. Rehr and S.D. Conradson, Phys. Rev. B **58**, 7565 (1998).
 - [16] J.A. Gupta et al., J. Cryst. Growth **242**, 141 (2002).
 - [17] W.R.L. Lambrecht *et al.* Phys. Rev. B **55**, 2612 (1997).
 - [18] M. Katsikini et al., Phys. Rev. B **56**, 13380 (1997).
 - [19] M. Brown et al., Phys. Rev. B **15**, 738 (1977).
 - [20] B. Gil and H. Mariette, Phys. Rev. B **35**, 7999 (1987).
 - [21] J. Neugebauer et al., Phys. Rev. B **51**, 10568 (1995).
 - [22] J.A. Gupta et al., J. Cryst. Growth **231**, 48 (2001) and references therein.
 - [23] T. H. Myers et al., J.Vac.Sci.Technol. B **17**, 1654 (1999)